Electrical conduction through a monatomic surface step

I. Matsuda[1,*], T. Hirahara[1], M. Ueno[1], R. Hobara[1] and S. Hasegawa[1]

[1] *Department of Physics, School of Science, the University of Tokyo, 7-3-1 Hongo, Bunkyo-ku, Tokyo 113-0033, Japan*

Abstract. We have succeeded in measuring resistance across a single atomic step at electrical conduction through a monatomic-layer metal on a crystal surface. Using independent methods of direct electrical conductivity measurement with four-tip scanning tunneling microscope probes and scanning tunneling spectroscopy observation, the conductivity across a monatomic step was found to be about $5 \times 10^3 \, \Omega^{-1} \mathrm{m}^{-1}$. Through analyses of the Landauer formula for 2D conductors and the recent theoretical calculations, the electron transport across an atomic step is fairly modeled as a tunneling process. Important formulas of surface conductivity developed by the present research are given.

1. INTRODUCTION

Surface superstructures prepared by metal adsorption on semiconductor surfaces have now become important playgrounds to study various dynamics of low-dimensional phase transition or transport phenomena. [1, 2] Advantages of surface studies are that the electron density or atomic position is visually probed in atomic resolution with scanning probe microscopies. Furthermore, electronic states (Fermi surfaces) are also directly measured by means of angle-resolved photoemission spectroscopy (ARPES). Recently, (anisotropic) conductivity measurements of surface superstructures have become possible with state-of-the-art monolithic micro-four-point probes (MFPP) and four-tip scanning tunneling microscope (STM) probes. [3-5]

Electron transports are generally governed by electron-phonon couplings and impurity scatterings. Especially, low-dimensional electron gas has strong interactions with localized scatters and such electron-impurity scattering events are expected to play dominant roles in surface state transport phenomena. On crystal surfaces, atomic steps [6] are unavoidable defects, which become inevitable barriers or resistance for the carrier transport through the topmost atomic layers on crystals, Fig.1(a), (b). On the other hand, the scattering events lead, through interference, to an oscillatory local density of states (LDOS) or standing waves, Fig.1(c). Analyses of the LDOS oscillation provide information of the scattering phenomena such as energy dispersion and reflection phase shift. [7] Since reflection phase shift at a scatter is related with transmission through it, a research of a standing wave will lead to obtaining its conductivity. Using an isotropic two-dimensional (2D) metallic surface, Si(111) $\sqrt{3} \times \sqrt{3}$-Ag, [8-11] described below, we have examined the issue. In this research, we studied conductance of a single atomic step through detailed analyses on standing waves near the steps and surface transport measurements. Surface steps are imaged by scanning tunneling microscope and the LDOS's are mapped by scanning tunneling spectroscopy (STS). At various tip bias, standing waves near the steps were observed and their transmission coefficients were determined from the reflection phase shifts. Utilizing Landauer formula of 2D, conductance of a single atomic step is experimentally obtained. Then, we measured anisotropic conductance of the step-controlled Si(111) $\sqrt{3} \times \sqrt{3}$-Ag surfaces by micro-four-point probe method using independently driven four tip STM. [3, 5] The measured conductance showed good agreements to those determined from the standing waves.
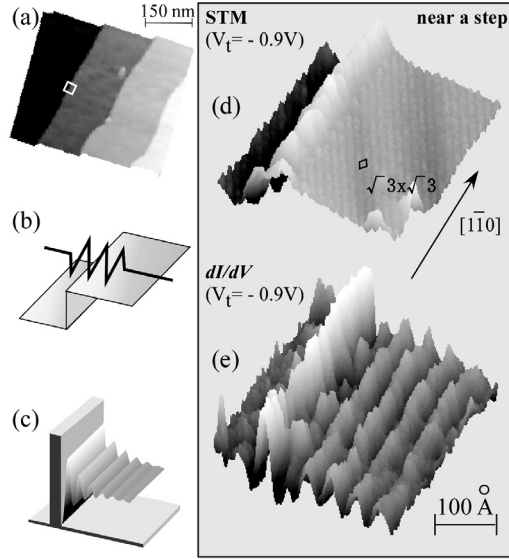
Figure 1. (a) A STM image of Si(111)$\sqrt{3} \times \sqrt{3}$-Ag on a flat wafer taken at room temperature. Steps are aligned parallel to the [1$\bar{1}$0] crystal axis. (b) The schematic resistance of a step. (c) Schematic drawing of the Friedel oscillation formed at the one-dimensional potential barrier. (d) A topographic (STM) image near a monatomic step, taken at 65 K with tip bias, V_t, of −0.9 V. A unit cell of $\sqrt{3} \times \sqrt{3}$ is shown. The STM region corresponds to the white box in (a). (e) A LDOS (dI/dV) image of the same area acquired at $V_t = -0.9$ V using lock-in detection.

2. PHOTOEMISSION FERMI AND BAND MAPPING

A Si(111)$\sqrt{3} \times \sqrt{3}$-Ag superstructure, induced by one monolayer (ML) Ag adsorption on a Si(111) crystal, has been one of the most popular, for which almost all kinds of surface-science techniques have been applied and its atomic and electronic structures are now well understood. [2] Figure 2 shows a gray-scale image of the Fermi surface and the band dispersion diagrams of the metallic surface state band (so-called the S_1 band) of Si(111)$\sqrt{3} \times \sqrt{3}$-Ag measured by ARPES. [8-11] The band dispersion images were taken along two crystal orientations ([11$\bar{2}$] and [1$\bar{1}$0]) around the $\bar{\Gamma}$ point. The Fermi surface of the S_1 band is a complete circle (Fermi ring) centered at the $\bar{\Gamma}$ point. The band dispersion curves in two directions are parabolic and cross Fermi level (E_F). It is clear, thus, that the S_1 band is an isotropic and metallic two-dimensional free-electron like.

Concerning the conductivity, while the Drude formula has been the simplest expression, here we show another simple formula derived from the 2-D Boltzmann equation, [8]

$$\sigma = (e^2/2) \cdot (\tau \cdot v_F) \cdot v_F \cdot D^{2D}. \tag{1}$$

where τ is the carrier relaxation time, v_F the Fermi velocity, and D^{2D} the 2D density of states at E_F. In the 2-D free electron model, D^{2D} and v_F can be expressed with Fermi wave vector (k_F) and effective mass (m^*) as $D^{2D} = m^*/\pi\eta^2$ and $v_F = \eta k_F/m^*$. These quantities can be determined from Fig.2 by elaborate analyses, including a newly developed 2D image fitting technique and they are $k_F \sim 0.1$ Å^{-1} and $m^* = 0.13m_e$ where m_e is the free electron mass. [10] Furthermore, τ can be evaluated from inelastic scattering time estimated from energy or momentum width of the band dispersion curve at Fermi level (Fig.2). [12] Detailed comparisons of temperature dependent τ between ARPES and conductivity results are reported elsewhere. [13] As described above, all the important transport parameters can be derived from photoemission spectroscopy and they are directly compared for ARPES and conductivity results on
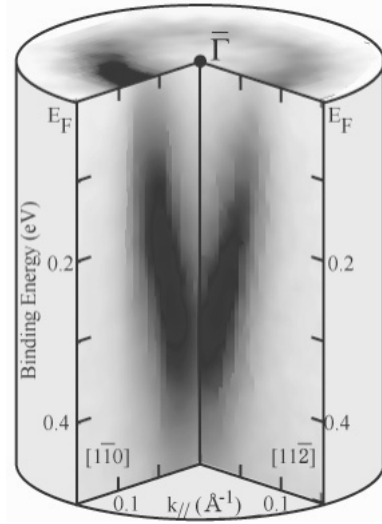
Figure 2. The experimentally measured Fermi surface and energy dispersion images of the metallic surface-state band of the Si(111)$\sqrt{3} \times \sqrt{3}$-Ag surface. $k_{//}$ is the length measured from the $\bar{\Gamma}$ point of the $\sqrt{3} \times \sqrt{3}$ surface Brillouin zone. The photoemission spectroscopy result has been taken with He Iα radiation.

bulk single crystals. [12] However, the comparison is not simple for a crystal surface because of surface steps, Fig.1(a).

3. TOPOGRAPHIC AND SPECTROSCOPIC IMAGE OF A MONATOMIC STEP

Figure 1(d, e) shows the STM and spectroscopic dI/dV images of the $\sqrt{3} \times \sqrt{3}$-Ag surface near an atomic step at 65 K. It can be seen that the $\sqrt{3} \times \sqrt{3}$-Ag surface superstructure almost extends up to the step edge. The LDOS modulation, standing wave (Friedel oscillation), in the dI/dV image [Fig.1(e)], has been well studied on noble metal surfaces. [7] The wavelength varied with tip bias, and the energy versus wave number dispersion obtained through the bias-dependent standing waves showed a parabola with an effective mass equal to that obtained by ARPES (Fig.2). [10, 11] The reflection phase shift, η, at the step edge is determined by fitting the dI/dV modulation, Fig.1(e), by a cosine function with a damping factor [7] at each tip bias. Around E_F, η is then determined to be about $- (0.8 \pm 0.05)\pi$. Once the reflection phase shift at a step is determined, the conductance through the step can be derived by combining a δ-potential model [14], Eq.(3), and the Landauer formula for the conductance of 2D conductor through 1D potential barrier, Eq.(4). The transmission coefficient T and the reflection phase shift η are related by

$$T = 1 - [1 + \tan^2(\eta + \pi)]^{-1}. \tag{3}$$

and

$$\sigma_{2D} = \frac{2e^2}{h} \cdot \frac{k_F}{\pi} \cdot T \quad [\Omega^{-1}\text{m}^{-1}] \tag{4}$$

where e, h and k_F are elementary charge, Planck's constant, and Fermi wavenumber, respectively. The δ-potential model quite suits to the present system since the concerned surface state is located in the bulk band gap and no carrier scattering of surface electrons into the bulk states occurs. [14] Inserting the experimentally determined η into the equation (3), T is determined to be 0.3 ± 0.15. The conduction electrons in the $\sqrt{3} \times \sqrt{3}$-Ag layer (surface state) pass through a step with a probability

of about 30%. Inserting T determined above and k_F ($\sim 0.1 \text{Å}^{-1}$) determined from the ARPES results [8-11], Fig.2, into the equation (4), the σ_{2D} at a monatomic step on this particular surface is determined to be $\sigma_{2D} = 9\,(\pm 4) \times 10^3 \Omega^{-1}\text{m}^{-1}$.

4. SURFACE CONDUCTIVITY MEASUREMENT WITH FOUR STM TIPS

For the direct determination of conductivity across the steps, we prepared the $\sqrt{3} \times \sqrt{3}$-Ag surface structure on a vicinal Si(111) crystal having a miscut angle of 0.9 or 1.8° toward [$\bar{1}\bar{1}2$] axis. Then, the electical measurements at room temperature were performed by so-called rotational square (RS) MFPP method [5] using the four-tip STM. This is a four-point probe resistance measurement in a square arrangement of the four probes with several tens μm probe spacing, Fig.3, and the square is rotated with respect to the sample surface. This RSMFPP method enables measuring anisotropic conductivity [5]. On our sample surface, all the steps are aligned along [$1\bar{1}0$] crystal axis and distributed uniformly with almost equal spacing (10~20 nm) over the surface, as judged from the STM observations (Fig.3). In micrometer scale, the vicinal surface can be regarded as an anisotropic 2D conductor because of the aligned step array; the conductivity in a direction perpendicular to the steps should be lower than that in
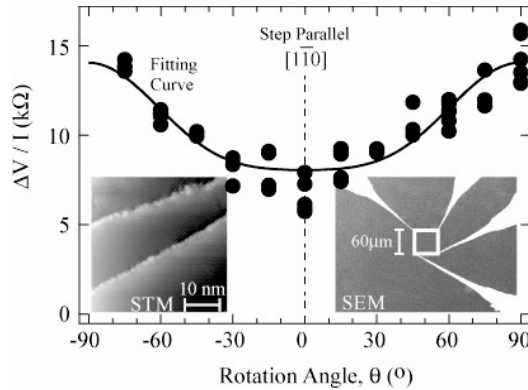
Figure 3. Resistance measured as a function of the rotation angle in the rotational square micro-four-point probe (RSMFPP) method for the $\sqrt{3} \times \sqrt{3}$-Ag surface on a vicinal Si(111) wafer (*n*, 1-10 Ωcm) with a miscut angle of 1.8° at room temperature. The probe spacing (a side of the square) was 60 μm. Experimental data are fitted by a function described in ref. [5]. (Left Inset) A STM image of the sample surface. (Right Inset) A scanning electron microscope (SEM) image of the four STM tips during the direct transport measurement.

step-parallel direction. Therefore, any anisotropy in conductivity detected by the RSMFPP measurement should be attributed to the steps, and then we can determine the resistance caused by atomic steps directly from it. This is because any channels for electrical conduction near the surface (surface-state bands on the topmost atomic layers, bulk-state bands in a surface space-charge layer beneath the surface, and bulk-state bands in the inner crystal) are isotropic. Resistance of the $\sqrt{3} \times \sqrt{3}$-Ag surface on a 1.8° miscut wafer is shown in Fig.3 as a function of rotation angle of the square with respect to [$1\bar{1}0$] crystal orientation. By fitting the results with a formula derived from the Poisson equation [5], we obtained sheet conductivities parallel ($\sigma_{//}$) and perpendicular ($\sigma_\perp$) to the step direction separately; $\sigma_{//}$ and $\sigma_\perp$ are 23×10^{-6} and $14 \times 10^{-6}\,\Omega^{-1}\text{K}^{-1}$, respectively, so that the anisotropy is $\sigma_{//}/\sigma_\perp \sim 1.6$. For a sample with a smaller miscut angle of the crystal surface, we acquired a smaller anisotropy because of a lower step density. The conductivity across a step of unit length σ_{step} ($\Omega^{-1}\text{m}^{-1}$) can be related with the sheet conductivities $\sigma_{//}$ and $\sigma_\perp$ by

$$N_{step}/\sigma_{step} = 1/\sigma_\perp \cdot 1/\sigma_{//} \qquad (5)$$

where N_{step} (m^{-1}) is the step density on the sample surface. Our vicinal Si(111) wafer with a miscut angle of $1.8°$ has $N_{step} \sim 10^8$ m^{-1}. Therefore we get $\sigma_{step} \sim 3 \times 10^3 \Omega^{-1} m^{-1}$. The σ step reasonably matches to the σ_{2D} obtained by the independent methods of dI/dV (STM) observations described before! It is noted that the similar value has also been acquired from direct electrical measurement by monolithic MF4PP on a step-controlled surface. [15]

5. SUMMARY

It is now obvious that conductance across a monatomic step on the $\sqrt{3} \times \sqrt{3}$-Ag surface is about 5×10^3 $\Omega^{-1} m^{-1}$. When electrical current flows through a step of 1cm, 1mm, 1μm, and 1nm long, the resistance across the step should be 0.02, 0.2, 200, and $2 \times 10^5 \Omega$. The resistance is negligible in macroscopic scale, but very critical in nanometer scale. Within the experimental error, the reasonable agreements among the independent methods indicate that electron transport through a monatomic step is fairly modeled as an electron tunneling process. Recent theoretical calculation have shown that the tunneling process through a monatomic step separating two $\sqrt{3} \times \sqrt{3}$-Ag terraces is attributed to the continuation of surface electron wave and bulk evanescent wave. [16] On the other hand, the δ-potential model provides a product of potential barrier height and potential width, V_0 a, of the atomic step as $10 (\pm 6)$ eV Å. Assuming a as a bond length of bulk Si crystal (2.35 Å), the V_0 is $4.5 (\pm 2.5)$ eV. This implies that, at a step, carrier electrons in metallic overlayers on semiconductor substrates tunnel through an energy barrier corresponding to energy difference between the vacuum level and the Fermi level (work function). A potential barrier height of work function may be a good approximation to estimate conductance across an atomic step for other systems.

References

[1]   M. E. Davila, J. Avila, M. C. Asensio, and G. Le Lay, Surf. Rev. Lett. **10**, 981 (2003).
[2]   I. Matsuda, H. Morikawa, C.-H. Liu, S. Ohuchi, S. Hasegawa, T. Okuda, T. Kinoshita, C. Ottaviani, A. Cricenti, M. D'angelo, P. Soukiassian, and G. LeLay, Phys. Rev. B **68**, 085407 (2003).
[3]   I. Matsuda, M. Ueno, T. Hirahara, R. Hobara, H. Morikawa, and S. Hasegawa, Phys. Rev. Lett. **93**, 236801 (2004).
[4]   T. Tanikawa, I. Matsuda, T. Kanagawa, and S. Hasegawa, Phys. Rev. Lett. **93**, 016801 (2004).
[5]   T. Kanagawa, R. Hobara, I. Matsuda, T. Tanikawa, A. Natori, and S. Hasegawa, Phys. Rev. Lett. **91**, 036805 (2003).
[6]   M. Ueno, I. Matsuda, C. Liu, and S. Hasegawa, Jpn. J. of Appl. Phys. **42**, 4894 (2003).
[7]   P. Avouris, I.-W. Lyo, R. E. Walkup, and Y. Hasegawa, J. Vac. Sci. Technol. B **12**, 1447 (1994).
[8]   I. Matsuda, T. Hirahara, M. Konishi, C. Liu, H. Morikawa, M. D'angelo, S. Hasegwa, T. Okuda, and T. Kinoshita, Phys. Rev. B, in press.
[9]   T. Hirahara, I. Matsuda, and S. Hasegawa, e-J. of Surf. Sci. and Nanotechnology, **2**, 141 (2004).
[10] T. Hirahara, I. Matsuda, M. Ueno, and S. Hasegawa, Surf. Sci. **563**, 191 (2004).
[11] J. N. Crain, K. N. Altmann, C. Bromberger, and F. J. Himpsel, Phys. Rev. B **66**, 205302 (2002).
[12] Y.-D. Chuang, A. D. Gromko, D. S. Dessau, T. Kimura, and Y. Tokura, Science, **292**, 1509 (2001).
[13] I. Matsuda, C. Liu, T. Hirahara, M. Ueno, T. Tanikawa, and S. Hasegawa, (unpublished).
[14] L. Bürgi, O. Jeandupeux, A. Hirstein, H. Brune, and K. Kern, Phys. Rev. Lett. **81**, 5370 (1998).
[15] T. M. Hansen, K. Stokbro, O. Hansen, T. Hassenkam, I. Shiraki, S. Hasegawa, and P. Boggild, Rev. Sci. Instrum. **74**, 3701 (2003).
[16] K. Kobayashi, Surf. Sci. in press.